UDP Identification and Error Mitigation in ToA-Based Indoor Localization Systems using Neural Network Architecture

Mohammad Heidari, *Member, IEEE*, Nayef Ali Alsindi, *Member, IEEE*, and Kaveh Pahlavan, *Fellow Member, IEEE*

***Abstract*—Time-of-Arrival (ToA) based localization has attracted considerable attention for solving the very complex and challenging problem of indoor localization, mainly due to its fine range estimation process. However, ToA-based localization systems are very vulnerable to the blockage of the direct path (DP) and occurrence of undetected direct path (UDP) conditions. Erroneous detection of other multipath components as DP, which corresponds to the true distance between transmitter and receiver, introduces substantial ranging and localization error into ToA-based systems. Therefore, in order to enable robust and accurate ToA-based indoor localization, it is important to identify and mitigate occurrence of DP blockage. In this paper we present two methodologies to identify and mitigate the UDP conditions in indoor environments. We first introduce our identification technique which utilizes the statistics of radio propagation channel metrics along with binary hypothesis testing and then we introduce our novel identification technique which integrates the same statistics into a neural network architecture. We analyze each approach and the effects of neural network parameters on the accuracy of the localization system. We also compare the results of the two approaches in a sample indoor environment using both real-time measurement and ray tracing simulation. The identification metrics are extracted from wideband frequency-domain measurements conducted in a typical office building with a system bandwidth of $500\,MHz$, centered around $1\,GHz$. Then we show that with the knowledge of the channel condition, it is possible to improve the localization performance by mitigating those UDP-induced ranging errors. Finally, we compare the standard deviation of localization error of traditional localization system and UDP identification-enhanced localization system with their respective lower bound.**

***Index Terms*—NLoS identification, UDP identification, ToA-based indoor localization, neural network architecture, binary hypothesis testing, wideband measurement.**

I. Introduction

LOCALIZATION using radio signals has attracted increasing attention in the field of positioning and tracking. The initial research studies resulted in a very accurate Global Positioning System (GPS) [1] which primarily was used for military applications and later broadly used for commercial and personal applications as well. However, research studies show that GPS's performance degrades drastically when receiver is located in indoor environment. This has motivated researchers to direct their efforts toward indoor localization systems and variety of solutions are widely discussed in literature.

Multitude applications of indoor localization systems range from commercial to military. In commercial domain, indoor localization has been considered for supply-chain and asset management. It has also been used in health care domain to locate and/or track elderly people and people with special needs as well as locating medications and instruments in hospitals. There also exist applications of indoor localization systems in public safety and military domains to locate fire fighters in under-fire buildings and soldiers located in indoor environment [2].

Indoor localization systems face complications in determining user's location mainly due to harsh wireless propagation environment in such areas. The indoor radio propagation channel is characterized as site-specific, exhibiting severe multipath and low probability of line of sight (LoS) signal propagation between the transmitter and receiver [3], making accurate indoor localization very challenging and necessitates novel approaches in their respective model design.

The existing models readily available in literature for the behavior of the ToA in indoor environment were developed for telecommunication purposes and hence they do not reflect the behavior of ToA used for localization purposes. In telecommunication applications the behavior of the ToA of different paths was used to estimate the multipath spread of the channel [4] while ToA-based indoor localization systems use the behavior of one component, the direct path (DP), to determine the distance between the transmitter and receiver. The erroneous detection of DP results in ranging error between the antenna pair which consequently degrades localization accuracy. The detection of DP, hence, divides the channel profiles into channel profiles with detected direct path (DDP) conditions which can be used for localization and channel profiles with undetected direct path (UDP) conditions which can not be used for localization [5].

Previous studies for identification of class of receiver location (NLoS identification) in cellular domain has been carried out in [6], [7] where they focused on rural and suburban scenarios. In indoor environment, however, the problem of modeling the channel and its propagation parameters becomes

Manuscript received March 29, 2008; revised December 3, 2008; accepted March 28, 2009. The associate editor coordinating the review of this paper and approving it for publication was D. Zeghlache.

The authors are with the Center for Wireless Information Network Studies, ECE Dept., Worcester Polytechnic Institute, 100 Institute Rd., Worcester, MA 01609 (e-mail: {mheidari, nayefalsindi}@gmail.com; kaveh@wpi.edu).

Digital Object Identifier 10.1109/TWC.2009.080415

more challenging [3]. Research studies for NLoS identification report successful identification of such scenarios [8], [9] in indoor environment. They also propose ranging error mitigation algorithms to improve the accuracy of the localization algorithm [9], [10]. Their research efforts, however, is focused on the problem of NLoS rather than UDP identification and they utilize channel models rather than real-time channel profiles obtained from measurements.

In this paper we propose two UDP identification approaches using binary hypothesis testing and an application of neural network architecture (NNA) design. Previously, NNAs are exploited in the field of localization and tracking. Power measurements from different access points can be used to form an NNA for location estimation [11], while [12] utilizes variety of propagation parameters to form and train the NNA for location purposes. The input parameters to the identification algorithms use propagation parameters obtained from wideband frequency-domain measurements conducted in a typical office environment. Our original research on neural network based UDP identification was published in [13] and this paper is a continuation and extension of our previous work. In this paper, the propagation parameters of the radio signal are initially used to form the likelihood functions, and hence, to construct and train the NNA as well as to initialize the binary hypothesis testing likelihood functions for both real-time measurement scenario and simulation. The effects of various NNA parameters on the performance of the sample localization system are studied as well as various scenarios in indoor environment to analyze the effectiveness of the proposed approach to improve the accuracy of the localization system. In addition, the results of traditional localization system and NNA-based localization system are compared with the theoretical Cramér-Rao bound of localization in the sample environment.

The paper is organized as following; section II discusses the basics of ToA-based localization and calculation of the Cramér-Rao bound of localization for any scenario. Section III explains the radio propagation parameters of a channel profile to be used for UDP identification and their respective modeling and distributions. Section IV is dedicated to detailed description of our identification approaches using binary hypothesis testing and neural network along with the effects of their parameters on the accuracy of the system. Section V describes the performance of binary hypothesis testing and NNA when applied to UDP identification problem, and performance of both traditional localization system and improved localization system using UDP identification and ranging error mitigation. Finally, section VI concludes the paper.

II. Indoor Localization Algorithms and Bounds

A. ToA-Based Ranging

The ideal indoor channel profile in the presence of multipath phenomenon is characterized as

$$h(t,\theta) = \sum_{k=1}^{L_p} \alpha_k s(t-\tau_k, \theta-\theta_k) \tag{1}$$

where $s(.)$ represents the time-domain pulse shape of the filter, L_p is the number of multipath components (MPCs), $\alpha_k = |\alpha_k| e^{j\phi_k}$ represents the amplitude and phase of the k^{th} path, τ_k represents the time delay of the k^{th} path and θ_k is the AoA of the k^{th} path [14].

In ToA-based localization systems, ToA of the DP of the received signal is used to estimate the distance of the antenna pair using time of flight between transmitter and receiver [15], $d_{DP} = \tau_{DP} \times c = \tau_1 \times c$, where d_{DP} represents the distance of the antenna pair, c represents the speed of light, and τ_{DP} represents the ToA of the DP. In order to estimate τ_{DP} we apply a peak detection algorithm to the filtered channel profile which results in detecting the first detected peak (FDP) and its respective ToA. The ToA of FDP, τ_{FDP}, is then used to approximate the distance of the antenna pair, $d_{FDP} = \tau_{FDP} \times c$, where d_{FDP} is the estimate of the distance of the antenna pair and τ_{FDP} represents the estimate of the τ_{DP}. The erroneous detection of the DP component results in ranging error, ε_d, which can then be defined as

$$\varepsilon_d = d_{FDP} - d_{DP} \tag{2}$$

In LoS conditions and mild multipath environment, the estimate, d_{FDP}, is typically very close to d_{DP} which results in negligible ranging error values. However, in heavy multipath environments, i.e. indoor environments, and NLoS conditions erroneous detection of the DP component typically results in very large ranging errors [16]. The ranging error caused by multipath is inversely proportional to the bandwidth of the measurement system and can be combated with increase of the bandwidth [16]. In NLoS conditions, due to the obstruction of DP component it may not be detected at the receiver side. Therefore, the performance of the localization system in such conditions extremely depends on the detection of the DP component which divides these conditions into two major classes of DDP and UDP. UDP errors are considered to be the dominant source of ranging error in indoor environment.

In this research we categorize the receiver locations into two main classes of DDP and UDP where the former refers to those receiver locations with small ranging errors while the latter refers to the receiver locations with unexpected large ranging error.

This classification provides us two hypotheses

$$\begin{cases} H_0 : DDP \mid d_{FDP} \approx d_{DP}, \varepsilon_d \approx 0 \\ H_1 : UDP \mid d_{FDP} \gg d_{DP}, \varepsilon_d \gg 0 \end{cases} \tag{3}$$

where H_0 denotes the DDP hypothesis, which indicates that ranging error is small and channel profile can effectively be used for localization, and H_1 denotes the UDP hypothesis, which indicates that ranging error is larger than its threshold and channel profile is not appropriate for being used in localization purposes.

B. Least Square Solution to Indoor Localization Problem

In 2-D localization, knowledge of three accurate distance measurements from three known reference points (RPs) will be sufficient to accurately locate the mobile terminal with the help of trilateration. Assume $[x_r \quad y_r]$ is the estimate of the coordinates of the mobile terminal. Furthermore, assume $[x_i \quad y_i]$ is the coordinate of the i^{th} RP. The distance between the i^{th} RP and mobile terminal can then be estimated as

$(x_r - x_i)^2 + (y_r - y_i)^2 = d_{FDP}^2$, where estimated distance is defined as $d_{FDP} = d_{DP} + \varepsilon_d$. This ranging error term includes three different ranging error contributors from physical measurement. As shown in [17], the major contributors can be modeled as $\varepsilon_d = \varepsilon_{UDP} + \varepsilon_m + \varepsilon_{pd}$, where ε_{UDP}, ε_m, and ε_{pd} represent blockage of DP, multipath, and propagation delay induced errors, respectively. ε_{pd} is assumed to be insignificant for indoor environment while ε_m is shown to follow a normal distribution, $\mathcal{N}(0, \sigma_\omega^2)$, where its variance, σ_ω^2, decreases with the increase of bandwidth and is shown to be sufficiently small for the bandwidths greater than $200\ MHz$ [16]. The term ε_{UDP} does not exist if the mobile terminal is in DDP conditions; however, in UDP conditions it can be observed that the infrastructure of the indoor environment commonly obstructs the DP component and causes unexpected larger ranging errors. As a result, the statistical characteristics of the ranging error in UDP class exhibits a heavy tail in its distribution function. This heavy tail phenomenon has been reported and modeled in the literature; in [18], [19] the observed ranging error was modeled as a combination of a Gaussian distribution and an exponential distribution; [20], [21] model the ranging error with a log-normal distribution, and finally [17], [22] model the behavior of ranging error in harsh NLoS environment with Generalized Extreme Value (GEV) distribution. In this paper, for simplicity, we will model the term ε_{UDP} with a normal random variable with known statistics as reported in [23].

In traditional localization systems, one approach is to estimate the receiver position using the least-squares (LS) algorithm to solve the trilateration equations. The particular instance of the LS algorithm that has been used for our evaluations is the one by Davidon [24], which attempts to minimize the objective function

$$f(\mathbf{x}) = \sum_{j=1}^{N} \left(d_j - \sqrt{(x_r - x_j)^2 + (y_r - y_j)^2} \right)^2 \qquad \mathbf{x} = [x_r \quad y_r] \tag{4}$$

in an iterative manner using the relation $\mathbf{x}_{k+1} = \mathbf{x}_k - \mathbf{H}_k \mathbf{g}(\mathbf{x}_k)$, where $\mathbf{H}_k$ represents an approximation to the inverse of the Hessian of $f(\mathbf{x})$, $\mathbf{G}(\mathbf{x})$, and $\mathbf{g}(\mathbf{x})$ is the gradient of $f(\mathbf{x})$, defined as $\mathbf{g}(\mathbf{x}) = \nabla f(\mathbf{x})$. The following relation defines when the computations will be terminated, $\rho_k = (\mathbf{g}(\mathbf{x}_{k+1}))^T \mathbf{H}_k (\mathbf{g}(\mathbf{x}_{k+1}))$, so that the iterations will stop when $\rho_k \leq \epsilon$, where ϵ is a small tolerance value.

C. Cramér-Rao Lower Bound on Localization Error in NLoS Environments

Cramér-Rao lower bound (CRLB) is an analytical lower limit for the variance or covariance matrix of any unbiased estimate of an unknown parameter(s) [25], [26]. It can be shown that for ToA-based localization algorithms the maximum likelihood estimator of the receiver is an asymptotically unbiased estimate when sufficient conditions are met. Therefore, the CRLB can be considered as an appropriate reference for the localization accuracy [27].

Define vector $\boldsymbol{\theta}$, the vector to be estimated, as $\boldsymbol{\theta} = [x_r \quad y_r \quad \varepsilon_1 \quad \varepsilon_2 \quad \varepsilon_3]$, where $\varepsilon_i = d_{FDP_i} - d_{DP_i}$. If $\hat{\boldsymbol{\theta}}$ is an estimate of $\boldsymbol{\theta}$, the CRLB can be defined as the inverse of the Fisher information matrix (FIM) as

$$E_{\boldsymbol{\theta}}[(\hat{\boldsymbol{\theta}} - \boldsymbol{\theta})(\hat{\boldsymbol{\theta}} - \boldsymbol{\theta})^T] \geq \mathbf{J}_{\boldsymbol{\theta}}^{-1} \tag{5}$$

where $\mathbf{A} > \mathbf{B}$ should be interpreted as matrix $(\mathbf{A} - \mathbf{B})$ is non-negative definite, and $E_{\boldsymbol{\theta}}[.]$ operation is interpreted as the expectation operation conditioned on $\boldsymbol{\theta}$. In localization systems, we are specifically interested in the first two diagonal elements of the CRLB as they provide the minimum mean-square error (localization error) of the position estimate $\mathbf{x} = [x_r \quad y_r]$

$$E(\hat{\theta}_b - \theta_b)^2 \geq [\mathbf{J}_{\boldsymbol{\theta}}^{-1}]_{bb}, \qquad \text{for} \qquad b \in 1, 2 \tag{6}$$

In case of our research studies, statistics of ε are available *a priori*. This leads to higher localization accuracy. The accuracy limit can then be obtained by the generalized CRLB (G-CRLB) [25]. In G-CRLB the information matrix consists of two components $\mathbf{J} = \mathbf{J}_{\boldsymbol{\theta}} + \mathbf{J}_\varepsilon$, where $\mathbf{J}_{\boldsymbol{\theta}}$ represents the information matrix corresponding to the receiver locations and measurements and $\mathbf{J}_\varepsilon$ represent the information matrix corresponding to the statistics of ranging error in UDP conditions. The FIM components can then be obtained as

$$\mathbf{J}_{\boldsymbol{\theta}} \overset{def}{=} E_{\boldsymbol{\theta}}[\frac{\partial}{\partial \boldsymbol{\theta}} \ln f(d_{FDP}|\boldsymbol{\theta}).(\frac{\partial}{\partial \boldsymbol{\theta}} \ln f(d_{FDP}|\boldsymbol{\theta}))^T] \tag{7}$$

where $f(d_{FDP}|\boldsymbol{\theta})$ is the joint probability density function (PDF) of d_{FDP_i} conditioned on $\boldsymbol{\theta}$, and

$$\mathbf{J}_\varepsilon \overset{def}{=} E_{\boldsymbol{\theta}}[\frac{\partial}{\partial \boldsymbol{\theta}} \ln p_{\boldsymbol{\theta}}(\boldsymbol{\theta}).(\frac{\partial}{\partial \boldsymbol{\theta}} \ln p_{\boldsymbol{\theta}}(\boldsymbol{\theta}))^T] \tag{8}$$

The slight difference between the FIM components in our study is the introduction of UDP conditions in addition to the NLoS conditions. In our studies the mobile terminal is always in NLoS conditions, but the condition can further be divided into DDP and UDP conditions as described in Eqn. (3). Therefore; The FIM components can then be evaluated as the following [27]

$$\mathbf{J}_{\boldsymbol{\theta}} = \begin{pmatrix} \mathbf{H}_{UDP}\boldsymbol{\Lambda}_{UDP}\mathbf{H}_{UDP}^T + \mathbf{H}_{DDP}\boldsymbol{\Lambda}_{DDP}\mathbf{H}_{DDP}^T & \mathbf{H}_{UDP}\boldsymbol{\Lambda}_{UDP} \\ \boldsymbol{\Lambda}_{UDP}^T\mathbf{H}_{UDP}^T & \boldsymbol{\Lambda}_{UDP} \end{pmatrix} \tag{9}$$

where $\mathbf{H}_{UDP}$ and $\mathbf{H}_{DDP}$ contain the geometry information of the localization scenarios and $\boldsymbol{\Lambda}_{UDP}$ and $\boldsymbol{\Lambda}_{DDP}$ contain the information of the measurement.

Additionally, $\mathbf{J}_\varepsilon$ can be represented as

$$\mathbf{J}_\varepsilon = \begin{pmatrix} \mathbf{0} & \mathbf{0} \\ \mathbf{0} & \boldsymbol{\Omega}_\varepsilon \end{pmatrix} \tag{10}$$

where

$$\boldsymbol{\Omega}_\varepsilon \overset{def}{=} E_{\boldsymbol{\varepsilon}}[\frac{\partial}{\partial \boldsymbol{\varepsilon}} \ln p_{\boldsymbol{\varepsilon}}(\boldsymbol{\varepsilon}).(\frac{\partial}{\partial \boldsymbol{\varepsilon}} \ln p_{\boldsymbol{\varepsilon}}(\boldsymbol{\varepsilon}))^T] \tag{11}$$

The final $\mathbf{J}$ matrix can then represented as

$$\mathbf{J}_{\boldsymbol{\theta}} = \begin{pmatrix} \mathbf{H}_{UDP}\mathbf{\Lambda}_{UDP}\mathbf{H}_{UDP}^T + \mathbf{H}_{DDP}\mathbf{\Lambda}_{DDP}\mathbf{H}_{DDP}^T & \mathbf{H}_{UDP}\Lambda_{UDP} \\ \mathbf{\Lambda}_{UDP}^T\mathbf{H}_{UDP}^T & \mathbf{\Lambda}_{UDP} + \mathbf{\Omega}_{\varepsilon} \end{pmatrix} = \begin{pmatrix} \mathbf{Y} & \mathbf{V} \\ \mathbf{V}^T & \mathbf{Z} \end{pmatrix} \tag{12}$$

Therefore, it can be shown that the G-CRLB can be represented by

$$[\mathbf{J}^{-1}]_{2\times 2} = [Y^{-1} + Y^{-1}V(\mathbf{\Omega}_{\varepsilon} + \mathbf{\Lambda}_{UDP} - V^T Y^{-1} V)^{-1} V^T Y^{-T}] \tag{13}$$

where $[\mathbf{J}^{-1}]_{2\times 2}$ represents the accuracy limit of the position estimates [27]. The G-CRLB can be deterministically described with *a priori* knowledge of receiver and transmitter locations and statistics of ranging error used for DDP/UDP conditions.

III. Channel Statistics for UDP Identification

Metric Definitions and Statistics

Propagation parameters of the radio signal have been previously used for variety of applications in telecommunications [3]. In this section we examine time and power characteristics of the radio signal to examine their effectiveness in identifying UDP conditions. A hybrid metric consisted of both time delay and power characteristics can also be used for UDP identification.

1) Time Metrics: The time characteristics of channel profiles have been used in literature for variety of applications. RMS delay spread and mean excess delay are being used to determine the data-rate in the communication systems [28]–[30]. Here, we utilize the time characteristics to identify the UDP condition.

- RMS delay spread

Amongst all of the delay metrics the RMS delay spread of the channel profile is one of the easiest to find and perhaps the most effective metric, relatively, to efficiently identify the UDP conditions. RMS delay spread is defined as the

$$\tau_{rms}^2 = \frac{\sum_{i=1}^{L_p} (\hat{\tau}_i - \tau_m)^2 |\alpha_i|^2}{\sum_{i=1}^{L_p} |\alpha_i|^2} \tag{14}$$

where $\hat{\tau}_i$ and α_i represent the ToA and complex amplitude of the i^{th} detected peak, respectively, L_p represents the number of detected peaks, and τ_m is the mean excess delay of the channel profile defined as

$$\tau_m = \frac{\sum_{i=1}^{L_p} \hat{\tau}_i |\alpha_i|^2}{\sum_{i=1}^{L_p} |\alpha_i|^2} \tag{15}$$

Conceptually, it can be observed that profiles with higher RMS delay spread are more likely to be in UDP conditions.

Constructing a database of DDP and UDP channel profiles and extracting their propagation metrics enable us to compare the statistics of the desired metric for both DDP and UDP conditions. Comparing the probability plots and probability distributions of the extracted RMS delay spread for DDP and UDP conditions further highlights the differences between the two cases as it is illustrated in Fig. 1 in which the τ_{rms} values are converted to distances [13]. The probability plots of the distribution of DDP and UDP clearly indicates that they can be best modeled with normal distribution and their separation indicates that their normal distribution parameters are distinct which follows

$$\begin{cases} p(\tau_d|H_0) = \frac{1}{\sqrt{2\pi}\sigma_d} \exp[-\frac{(\tau_d - \mu_d)^2}{2\sigma_d^2}] \\ p(\tau_u|H_1) = \frac{1}{\sqrt{2\pi}\sigma_u} \exp[-\frac{(\tau_u - \mu_u)^2}{2\sigma_u^2}] \end{cases} \tag{16}$$

where μ_d and σ_d represent the mean and standard deviation of the normal distributions of the channel profiles associated with DDP conditions. Similarly, μ_u and σ_u represent the mean and standard deviation of the normal distribution of the channel profiles associated with UDP conditions. In order to quantitatively determine the goodness-of-fit of the data to the normal distribution we apply the Kolmogorov-Smirnov $(K-S)$ and χ^2 hypothesis tests. Both tests are performed at 5% significant level to obtain the passing rates of the proposed distribution. The results of the normal distribution parameters, $K-S$ test and χ^2 test are summarized in Table I. It can be observed that normal distribution passes the assumption of normality. It is worth mentioning that the other measures of time delay characteristics of channel profile are found to be not as effective to our classification.

2) Power Metrics: The other class of metrics that can be extracted from the channel profile are power characteristics such as total power and FDP power.

- Total Power (RSS)

RSS is a simple metric that is easily measured by most wireless devices. For example, the MAC layer of IEEE 802.11 WLAN standard provides RSS information from all active access points (APs) in a quasi-periodic beacon signal that can be used as a metric for localization [15]. Total power is then represented by

$$P_{tot} = -r = 10\log_{10}(\sum_{i=1}^{L_p} |\alpha_i|^2) \tag{17}$$

For identification, power loss or $-P_{tot}$ can be used instead. It can be observed that profiles with higher power loss are more likely to be UDP conditions.

Similar to the RMS delay spread, we can distinguish the DDP conditions from the UDP conditions based on the total power of the observed channel profile. This is best illustrated in Fig. 2 in which their respective probability plots and their Weibull fits are sketched as well as probability distribution functions. According to our studies and based on the comparison of the goodness-of-fit for different distributions for modeling the total power, we chose Weibull distribution. The selection of the best distribution is performed by Akaike's

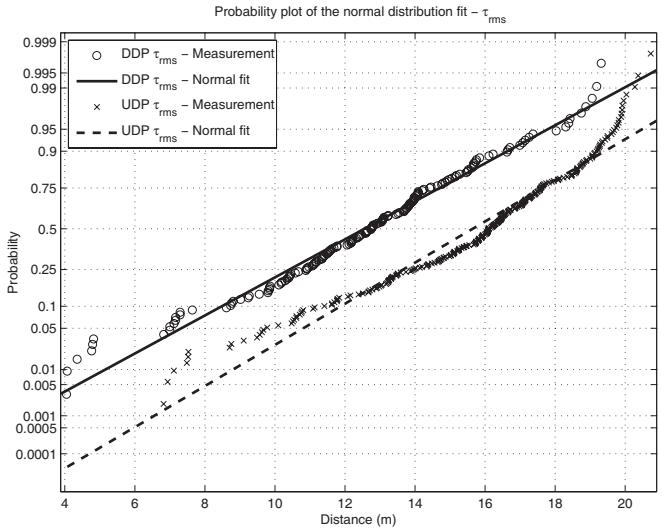

(a) Probability Plot

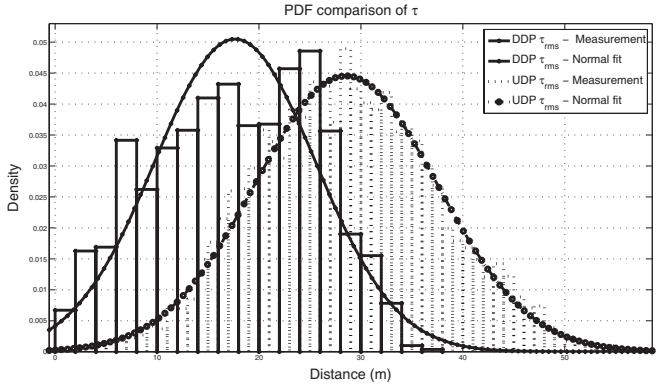

(b) Probability Distribution Function Plot

Fig. 1. Normality of τ_{rms} for DDP and UDP profiles.

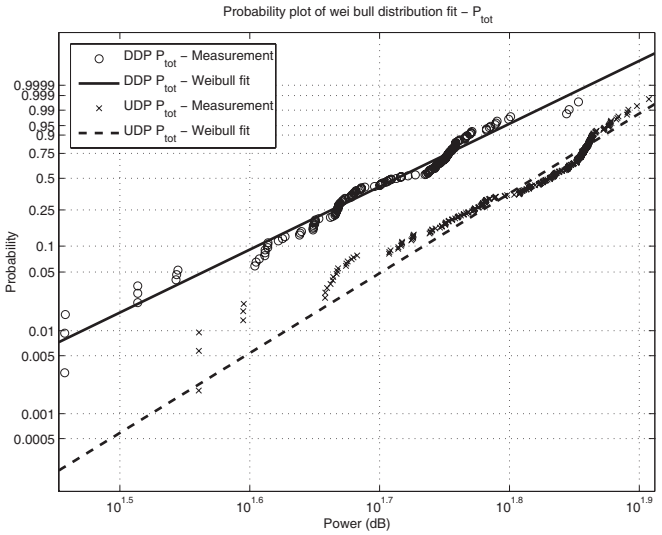

(a) Probability Plot

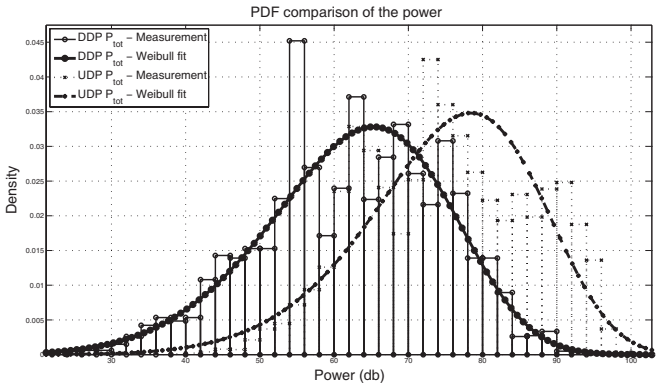

(b) Probability Distribution Function Plot

Fig. 2. Weibull distribution modeling of total power.

weights method. The separation of the curves illustrates the difference of the $-P_{tot} = r$ behavior for different DDP/UDP conditions [13]. The distributions can then be described as following

$$\begin{cases} p(r_d|H_0) = \frac{b_d}{a_d}(\frac{r_d}{a_d})^{b_d-1}\exp[-(\frac{r_d}{a_d})^{b_d}] \\ p(r_u|H_1) = \frac{b_u}{a_u}(\frac{r_u}{a_u})^{b_u-1}\exp[-(\frac{r_u}{a_u})^{b_u}] \end{cases} \quad (18)$$

where b_d and a_d represent the shape and scale parameters of the Weibull distribution associated with DDP channel profiles, respectively. Similarly, b_u and a_u represent the shape and scale parameters of the Weibull distribution associated with UDP channel profiles. Similar to RMS delay spread metric, in order to quantitatively determine the goodness-of-fit of the Weibull distribution to the data we apply the Kolmogorov-Smirnov $K-S$ and χ^2 hypothesis tests. The results of the Weibull distribution parameters, $K-S$ test and χ^2 test are summarized in Table I.

3) Hybrid Time/Power Metric: Although, each time or power metric can be used individually to identify the class of receiver locations, it is possible to form a hybrid metric to achieve better results in identification of the UDP conditions. Here, we propose to use a hybrid metric incorporating ToA of FDP component and its respective power as the metric to identify the UDP conditions. Mathematically, it is represented by

$$\xi_{hyb} = -P_{FDP} \times \tau_{FDP} \quad (19)$$

where ξ_{hyb} represents the metric being extracted.

Finally, by studying the hybrid metric gathered from DDP and UDP channel profiles it can be shown that the desired metric can be best modeled with Weibull distribution. Figure 3 represents the separation of the fits and proves that, indeed, the proposed metric can effectively be used in UDP condition identification. The corresponding equations can then be described as

$$\begin{cases} p(\xi_d|H_0) = \frac{\kappa_d}{\lambda_d}(\frac{\xi_d}{\lambda_d})^{\kappa_d-1}\exp[-(\frac{\xi_d}{\lambda_d})^{\kappa_d}] \\ p(\xi_u|H_1) = \frac{\kappa_u}{\lambda_u}(\frac{\xi_u}{\lambda_u})^{\kappa_u-1}\exp[-(\frac{\xi_u}{\lambda_u})^{\kappa_u}] \end{cases} \quad (20)$$

where κ_d and λ_d represent the shape and scale parameters of the Weibull distribution associated with DDP channel profiles, respectively. Similarly, κ_u and λ_u represent the shape and scale parameters of the Weibull distribution associated with UDP channel profiles. The results of $K-S$ and χ^2 tests for goodness-of-fit show close agreement for the assumption of the Weibull distribution. The results of the Weibull distribution parameters, $K-S$ test and χ^2 test are summarized in Table I [13].

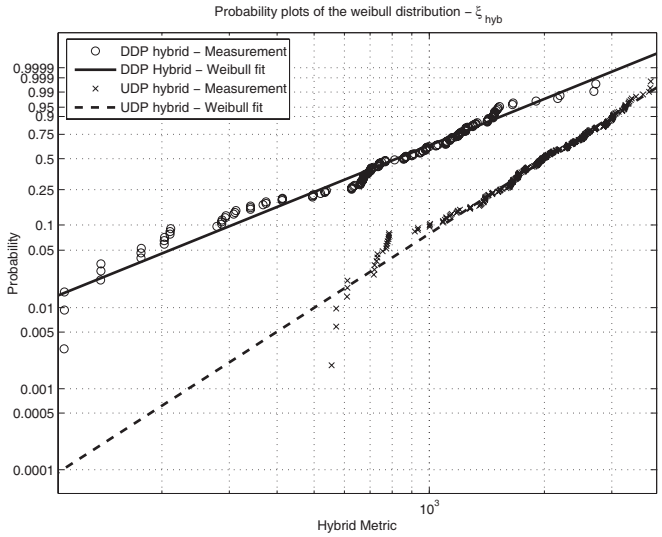

(a) Probability Plot

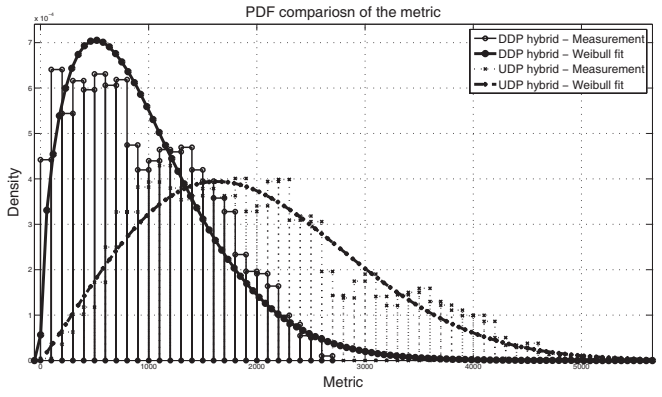

(b) Probability Distribution Function Plot

Fig. 3. Weibull distribution modeling of hybrid metric.

IV. UDP Identification Techniques

A. Binary Hypothesis Testing

Using the statistics of τ_{rms}, r, and ξ_{hyb} to identify the UDP conditions, the binary likelihood ratio tests can be performed to select the most probable hypothesis [9]. For this purpose, we picked a random profile and extracted its respective metrics. The likelihood function of the observed RMS delay spread, τ_{rms_i}, for DDP condition can then be described as

$$L(H_0|\tau_{rms_i}) = p(\tau_{rms_i}|H_0) = p(\tau_d)|_{\tau_d=\tau_{rms_i}} \tag{21}$$

Similarly, the likelihood function of the observed RMS delay spread, τ_{rms_i}, for UDP condition can then be described as $L(H_1|\tau_{rms_i}) = p(\tau_{rms_i}|H_1) = p(\tau_u)|_{\tau_u=\tau_{rms_i}}$.

The likelihood ratio function of τ_{rms} can then be determined as

$$\Lambda(\tau_{rms_i}) = \frac{\sup\{L(H_0|\tau_{rms_i})\}}{\sup\{L(H_1|\tau_{rms_i})\}} \tag{22}$$

The defined likelihood ratio functions are the simplified Bayesian alternative to the traditional hypothesis testing. The outcome of the likelihood ratio functions can be compared to a certain threshold, i.e. unity for binary hypothesis testing, to make a decision.

$$\Lambda(\tau_{rms_i}) \underset{H_1}{\overset{H_0}{\gtrless}} \eta_{rms} \tag{23}$$

Similarly, we can define the likelihood functions for P_{tot} and ξ_{hyb} as $\Lambda(r_i) = \frac{\sup\{L(H_0|r_i)\}}{\sup\{L(H_1|r_i)\}}$ and $\Lambda(\xi_i) = \frac{\sup\{L(H_0|\xi_i)\}}{\sup\{L(H_1|\xi_i)\}}$, which leads us to the corresponding hypothesis tests as $\Lambda(r_i) \underset{H_1}{\overset{H_0}{\gtrless}} \eta_r$ and $\Lambda(\xi_i) \underset{H_1}{\overset{H_0}{\gtrless}} \eta_\xi$.

Each of the above likelihood ratio tests can individually be applied for UDP identification of an observed channel profile. The outcome of the likelihood ratio test being greater than unity indicates that the receiver location is more likely to be a DDP condition and can appropriately be used in localization algorithm while the outcome less than unity indicates that the profile is, indeed, more likely to belong to UDP class of receiver location; hence, the estimated τ_{FDP} has to be mitigated before being used in the localization algorithm.

To use the likelihood functions more effectively, we can combine the likelihood functions and form a joint likelihood function. Assumption of the independence of the likelihood functions along with combining them leads to a suboptimal likelihood function defined as

$$\begin{aligned} \delta_{sim}(\tau_{rms}, P_{tot}, \xi_{hyb}) &= \Lambda_{sim}(\tau_{rms}, P_{tot}, \xi_{hyb}) \\ &= \Lambda(\tau_{rms}) \times \Lambda(P_{tot}) \times \Lambda(\xi_{hyb}) \end{aligned} \tag{24}$$

which can be compared to a certain threshold for decision making, i.e. $\Lambda_{sim}(\tau_{rms}, P_{tot}, \xi_{hyb}) \underset{H_1}{\overset{H_0}{\gtrless}} \eta_\delta$. The results of the accuracy of the likelihood hypothesis tests, individually and as a joint distribution, are summarized in Table II.

TABLE I
THE PARAMETERS OF DISTRIBUTIONS OF τ_{rms}, $-P_{tot}$, AND ξ_{hyb}

Channel Profile τ_{rms}	$\mu_{\tau_{rms}}$	$\sigma_{\tau_{rms}}$	$K - S_{\tau_{rms}}$	$\chi^2_{\tau_{rms}}$
DDP	12.55	3.18	94.30%	56.63%
UDP	15.64	2.94	89.02%	47.21%
Channel Profile $-P_{tot}$	a_P	b_P	$K - S_P$	χ^2_P
DDP	54.23	7.59	89.57%	29.72%
UDP	70.45	9.63	88.55%	30.63%
Channel Profile ξ_{hyb}	λ_m	κ_m	$K - S_m$	χ^2_m
DDP	995.05	1.90	91.00%	52.00%
UDP	2279.09	3.03	94.92%	87.25%

B. Neural Network Architecture

The results of individual binary hypothesis testing can be applied to the identification problem as well as the joint-parameter binary hypothesis testing. However, it is possible to combine the outcomes of the likelihood functions to form a simple NNA. The block diagram of such system is shown in Fig. 4. We can use the outputs of the likelihood functions as inputs to NNA. NNA will then consists of two layer, the hidden layer and output layer. The hidden layer consists of

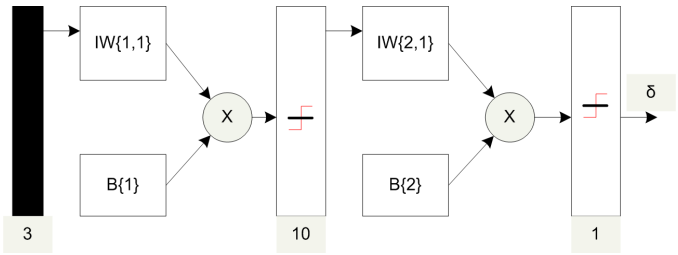

Fig. 4. Basic schematic of the artificial neural network used in this study. For training, the network is fed with the extracted RMS delay spread, total power, and hybrid metric of the channel profile as inputs as well as UDP identification flag as output. The process is repeated for few receiver location. Once NNA is trained, the extracted metric of an unknown channel profile is fed to the network and networks simulates the respective output. The process is repeated for all of the transmitters, individually but simultaneously.

$neurons$ and the output, δ_{meas}, can be used as a flag to indicate UDP conditions.

There exist several network types available in literature to construct the NNA [31]. Several examples of these types are feed-forward backdrop, cascade-forward backdrop, generalized regression, hopefield, and etc. The feed-forward backdrop type is chosen for this research [12].

In general, NNA forms a function of the inputs to obtain the output; in case of our UDP identification flag $\delta_{meas} = G_1(\sum_i \omega_i g_i(\mathbf{u}))$, where $G_1(.)$ is the predefined function and $\mathbf{u} = [\tau_{rms_i} \quad r_i \quad \xi_i]^T$ represents the input vector and ω_is represent the weights of the NNA. Each of the g_i components are themselves a function of the inputs of the NNA as $g_i(\mathbf{x}) = G_2(B_1\tau_{rms_i} + B_2 p_i + B_3\xi_i)$, where $G_2(.)$ is the inner predefined function and B_is are referred to as biases of the NNA.

The task of the NNA is to learn the pattern of the occurrence of UDP based on the training set of data which is available to the NNA at the training mode. In order to learn and adjust the weights and biases to solve the task in an optimal sense, we have to initially define a cost function for the network. The typical cost functions used in NNA are mean squared error (MSE), regularized mean squared error (MSEREG), and sum squared error (SSE) defined in [31]. The goal of NNA is to minimize the preferred cost function over the training input data. For better functionality of NNA and to prevent the weights and biases to grow exponentially, the input data are usually normalized to the range of $[0 \quad 1]$.

Training function of the NNA is another important aspect of NNA which affects the performance of the NNA. There exist various functions for training a feed-forward backdrop NNA such as Levenberg-Marquardt algorithm, conjugate gradient algorithms, and quasi-Newton algorithms. The difference between the algorithms are their speed, memory usage, and performance. Levenberg-Marquardt algorithm is shown to be one of the fastest algorithms while maintaining the performance at desired level [31].

After selecting the type of the NNA and training functions, feeding the NNA with samples of extracted metrics and desired UDP identification flags allows the network to adjust its weight and bias values to adapt to the pattern of UDP identification problem. In our study, we feed the NNA with samples of τ_{rms}, r, and ξ_{hyb} as inputs and binary target values of 1 and 0, 1 for the case of UDP condition and 0 for the case of DDP.

TABLE II
ACCURACY OF UDP IDENTIFICATION USING LIKELIHOOD HYPOTHESIS TESTS AND NEURAL NETWORK ARCHITECTURE

Likelihood Ratio	$CorrectDecision$
τ_{rms}	72.40%
P_{tot}	78.30%
ξ_{hyb}	85.48%
δ_{sim}	89.29%
δ_{meas}	92.00%

After training the NNA, we can simulate the unknown channel profiles by feeding their extracted τ_{rms_i}, r_i, and ξ_i to the NNA to identify the UDP condition. In one small experiment to compare the accuracy of the UDP identification using binary hypothesis testing and NNA we used 500 channel profile collected in our sample indoor environment. We used 400 of the channel profiles to obtain the statistics of the likelihood functions and their respective distribution parameters for binary hypothesis testing. We also used the same 400 channel profiles to train the NNA. We then compared the results of the UDP identification using binary hypothesis testing for a subset of channel profiles including all the 100 unknown channel profiles. We then used the same set of channel profiles in NNA for UDP identification. The results of individual binary hypothesis testings, joint-parameter binary hypothesis testing, and NNA are summarized in Table II.

It can be observed that amongst individual metrics, the hybrid metric performs superior, as expected, while the other two yield reasonable identification pointers. Combining all the individual binary hypothesis testings and forming the joint-parameter binary hypothesis testing results in better performance for UDP identification. In addition, the overall performance of NNA is superior than binary hypothesis testings, as the NNA has adapted itself to the classification problem and the weights are adjusted accordingly.

V. PERFORMANCE OF UDP IDENTIFICATION IN NLOS

A. Localization Scenario Setup

The localization scenario resembled a common scenario in indoor environment in which NLoS condition is very common. The wideband measurements were taken on the third floor of the Atwater Kent building at Worcester Polytechnic Institute. In addition to NLoS condition, two metallic shaft located on the third floor cause instant UDP conditions which make localization in such environments very challenging. The transmitter locations were chosen to create lots of UDP conditions as the mobile terminal moves along the receiver locations on the dashed line around the central loop of the floor plan. Figure 5 illustrates the location of the transmitters and receivers and presents a simple visualization of the UDP conditions.

1) Measurement Campaign: The measurement system consisted of vector network analyzer (VNA), monopole quarter wave antenna, low-noise amplifier and power amplifier. Measurements were taken from $750\,MHz$ to $1.25\,GHz$, centered around $1\,GHz$, to provide enough bandwidth to resolve the

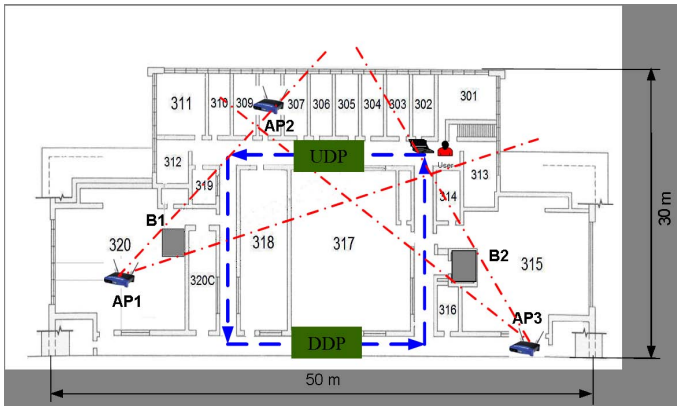

Fig. 5. Localization scenario - Three transmitter locations and 76 receiver locations around the central loop of the the third floor of AK Labs.

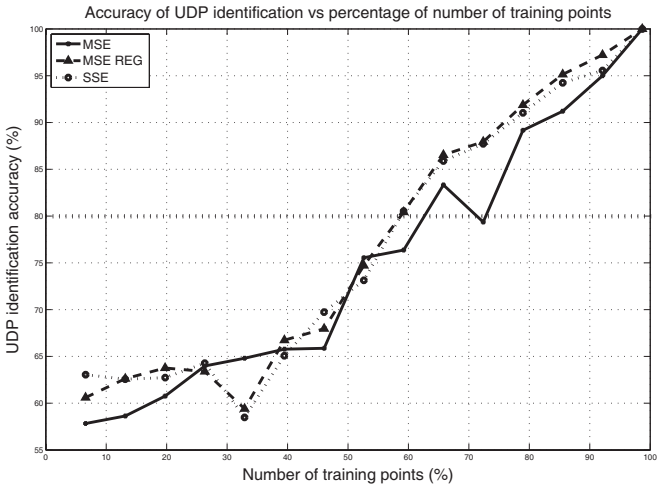

Fig. 6. Accuracy of UDP identification as a function of number of training points used to train the NNA.

MPCs. The results of the frequency-domain measurements were then post-processed in Matlab® to obtain the time-domain response using chirp-z method along with raised-cosine filter. Peak detection algorithm were then used to extract the MPCs, and consequently τ_{FDP} and other desired metrics. τ_{FDP} is then used to approximate the spacing of the antenna pair.

2) Simulation Campaign: For simulations, an internally developed ray tracing software has been used [32] and the output of this software has been processed by Matlab® by using Davidons least squares algorithm [24]. The floor plan of the scenario, i.e. third floor of AK Labs at WPI, was modified for the software to reflect the presence of the metallic objects in the floor plan, i.e. the metallic chamber and elevator shaft.

3) Neural Network Setup: Identifying the UDP scenarios with the aid of NNA gives us an edge to mitigate the ranging associated with the profile. For this purpose, we selected an NNA with feed-forward backdrop type and Levenberg-Marquardt algorithm. The NNA consisted of two layers with 10 neurons and 1 neuron, respectively. The output function of the hidden layer, i.e. the layer with 10 neurons, was adjusted to hyperbolic tangent sigmoid transfer function, i.e. $G_2(n) = \frac{2}{1+e^{-2n}} - 1$, while the output function of the second layer was linear transfer function, i.e. $G_1(n) = n$. The cost function to minimize was considered to be the MSE function. After training the network with few extracted metrics of the frequency-domain measurements of the sample receiver locations, we simulated the network with extracted metrics from channel profiles with unknown UDP identification flag. We used the outputs of the simulation as an UDP identification flag. If the output for a specific location was 0, we used the obtained d_{FDP} of the channel profile for localization. However, if the output of the NNA was 1, we considered the channel profile as UDP and remedied the respective d_{FDP} prior to using it for localization. In order to remedy the range estimate we subtracted a correction value from d_{FDP}. Since the exact value of the error is not known, the statistics of the ranging error [5], [23] in such conditions can be used to remedy the distance estimate, i.e. $\tau_{DP} \simeq \tau_{FDP} - \varepsilon_\tau$ or $d_{DP_i} \simeq d_{FDP_i} - \varepsilon_d$. In this case the range measurement is obtained based on physical layer measurements. In the case of obtaining the range measurement using MAC layer, additional sources of error are introduced in the system and have to be removed before proceeding to localization step.

B. NNA Parameters and Generalization of the Network

The performance of an NNA highly depends on its parameters with which it has been initialized. In this section we analyze the effects of number of training points on the overall performance of the NNA for the indoor localization problem. Similar to the previous experiment we train the NNA with few extracted metrics with known UDP identification flags so NNA can adjust its weights and biases. When a new profile is observed by the NNA, it simulates the output based on the previously adjusted weights and biases. To analyze the performance of the NNA with different sets of training points, we changed the number of training points of the NNA and recorded the performance of the network. Figure 6 illustrates the accuracy of predicting the UDP conditions as a function of number of training points for the three specified cost functions.

At first it can be observed that MSE with regularization performs the best. The small differences between the performance of the network when different cost functions are used are problem-specific. For different problems individual cost function might perform better. However, in the case of UDP identification using propagation parameters of the radio signal, the MSE cost function with regularization not only performed superior in terms of accuracy but also the convergence time of the network was considerably shorter than the other two. We measured the convergence time of the NNA in terms of epochs to be used to reach a flat cost function plot. In our experiment, MSE and SSE usually needed 50 to 100 epochs to reach the flat plot while MSE with regularization needed fewer epochs, usually in the order of 20 to 40. The target goal of the performance for each cost function is also an important parameter in pattern recognition. In our experiment we found that performance of 0.1 to 0.11 is desirable for such cost function as performances less than 0.1 cause overfitting of the network and performances more than 0.11 simply do not solve the pattern classification problem. In the case of MSE with regularization, target goal of 0.3 to 0.4 was desirable and

TABLE III
GENERALIZATION OF UDP IDENTIFICATION

Training Set	**Simulation Set**	Mean of Accuracy	Standard Deviation of Accuracy
Tx_1	Tx_2	73.68%	5.95%
Tx_1	Tx_3	77.31%	11.15%
Tx_2	Tx_1	71.31%	3.76%
Tx_2	Tx_3	67.88%	3.30%
Tx_3	Tx_1	74.20%	2.88%
Tx_3	Tx_2	77.36%	4.49%

SSE worked better with target goals in the order of 17 to 19.

It can also be observed that training the network with few training points results in poor UDP identification. However, even using as few as 10% of total receiver locations results in 60% accuracy in UDP identification. In our research, we chose to use almost 60% of the total receiver locations corresponding to one transmitter to train the network which results in 80% accuracy in UDP identification.

In another experiment we analyzed the performance of the NNA when generalized to different setup of transmitter and receiver. We used the propagation parameters of all the receiver locations corresponding to the first transmitter as the training set and simulated the UDP identification flag for the other transmitters. Since the scenario between the transmitter locations and receiver locations were completely different, this experiment could lead us to analyze the performance of the network when generalized to other transmitter locations and/or other buildings with similar interior characteristics. The experiment prove to be 75% accurate in predicting the UDP conditions when a completely different set of measurement in a similar indoor environment was used to train the network. It implies that the training phase of NNA can be conducted once and be used for different locations of the transmitter. The results of the experiment is reported in Table III.

C. Simulation and Results

The accuracy of an indoor localization system is drastically degraded when UDP conditions occurs. With the proposed methods to identify such conditions we are able to improve the accuracy of such systems. To illustrate the effectiveness of such methods, we setup two experiments in the described scenario and we analyze the results both in simulation and practice. The scenarios differ in the number of RPs used for localization. The measurement setup and simulation setup were described in V-A1 and V-A2. The reported RMSE value of localization error is found to be $8.42m$ for measurement and $5.94m$ for simulation. As can be verified from the scenario, the presence of two big metallic objects causes severe degradation to the accuracy of the localization system both in simulation and measurement. As was expected, localization with two RPs results in very inaccurate locations. It is worth mentioning that error values in measurement are typically larger than simulation as in measurements there exist several small metallic objects obstructing (or deflecting) the LoS component which are not reflected in simulation. These metallic objects can be referred to as micro-metallic objects such as metallic desks and shelves, metallic frames, and computer cases. Inclusion of all this details in simulation is not possible, hence, simulation results in smaller ranging errors.

In the next step, we examine the effects of UDP identification and ranging error mitigation associated with such cases on the accuracy of the localization system. For each receiver location, we extract the propagation parameters of the channel profile between the receiver location and each transmitter location and feed it to the previously trained NNA. The output of the NNA is used as a flag to decide if the channel profile is in UDP conditions. If the channel profile was in UDP condition, we remedy the distance estimate. The new RMSE values $3.53\,m$ for measurement system and $2.14\,m$ for simulation. As expected, employment of UDP identification and ranging error mitigation improved the accuracy of the localization system by 60%. It should be noted that the result of UDP identification is not 100% and there exist false alarms, i.e. DDP conditions which were identified as UDP. Nevertheless, UDP identification is able to enhance the accuracy of the indoor localization system.

The next experiment utilizes three RPs to locate the mobile terminal. The minimum number of RPs for 2-D localization is three, hence, intuitively we expect to observe improvements in the accuracy of the localization system. Using traditional localization system, the RMSE value of localization error was obtained to be $4.94\,m$ which shows 50% improvement compared to the case of two RPs. Repeating the same scenario for simulation setup yields $3.12\,m$ which again shows improvement over two RPs scenario. Now employing the UDP identification and ranging error mitigation approach, we repeat the scenario for both measurement and simulation. The measurement scenario with three RPs along with UDP identification results in RMSE value of $2.31\,m$ localization error which is another 60% improvement in the accuracy of the localization system. Likewise, simulation with three RPs along with UDP identification results in $1.56\,m$, again with exactly 50% improvement compared to traditional system. Figure 7 explains the results of the experiment. It can be observed that in both simulation and measurement the employment of UDP identification method improves the accuracy of the localization system as the located receiver locations are closer to their actual location. However, it can also be noted that simulation of localization systems in indoor environments sometimes outputs unrealistic results as not enough details of the building and obstacles can be simulated. In 50% of receiver locations, since there is no UDP condition, simulation results in the exact receiver location which in reality can not be achieved when real-time measurements are used. Therefore, it is very important to use realistic models for error in indoor environment and find solutions to remedy those errors as this paper describes.

Figure 8 compares the CDF of standard deviation of localization errors of the three RPs scenario, only for measurement with or without UDP identification, and it also compares the results with CRLB of the localization scenario using the three RPs setup. It can be observed that both in simulation and measurement, employing the UDP identification method along with ranging error mitigation can improve the accuracy of the indoor localization system. It can be also noted that

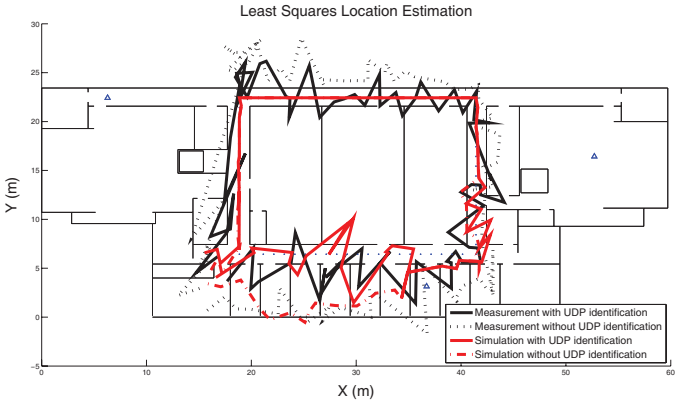

Fig. 7. Localization error in sample indoor environment for three RPs.

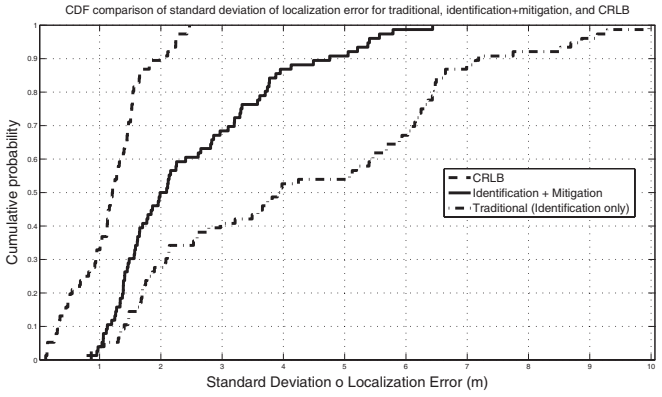

Fig. 8. CDF of localization error for the sample indoor environment for three RPs.

UDP identification makes it possible to attain the CRLB of localization error for the performance of the localization system.

VI. Conclusion

This research study has focused on the details of identification of the UDP conditions and mitigation of large ranging errors associated with such conditions in ToA-based indoor ranging problem. We have introduced two different novel methods to identify the UDP condition. The first approach uses statistics of channel propagation parameters to establish a binary hypothesis test and the second approach utilizes an application of neural networks to analyze the pattern of occurrence of UDP conditions. Pattern classification characteristics of the neural networks enable us to train the network with previously collected data and then used the trained network to identify the UDP condition when an unknown channel is presented. We have used power and time metrics obtained from various channel profiles to collect the statistics and ultimately to identify the occurrence of UDP condition. Both approaches are shown to be able to precisely identify the UDP condition. Once a UDP condition is spotted, the ranging error associated with it can be mitigated according to the statistics of ranging error in such conditions. The overall UDP identification and error mitigation can reasonably improve the accuracy of the indoor localization system both in simulation and practice.

References

[1] E. D. Kaplan, *Understanding GPS: Principles and Applications*, 1st ed. Boston: Artech House, 1996.

[2] A. H. Sayed, A. Tarighat, and N. Khajehnouri, "Network-based wireless location," *IEEE Signal Processing Mag.*, vol. 22, no. 4, pp. 24–40, May 1998.

[3] K. Pahlavan and A. H. Levesque, *Wireless Information Networks*, 2nd ed. New York: John Wiley & Sons, Inc., 2005.

[4] K. Pahlavan, P. Krishnamurthy, and J. Beneat, "Wideband radio propagation modeling for indoor geolocation applications," *IEEE Commun. Mag.*, vol. 36, no. 4, pp. 60–65, Apr. 1998.

[5] B. Alavi and K. Pahlavan, "Modeling of the distance measurement error using UWB indoor radio measurement," *IEEE Commun. Lett.*, vol. 10, no. 4, pp. 275–277, Apr. 2006.

[6] L. Cong and W. Zhuang, "Nonline-of-sight error mitigation in mobile location," *IEEE Trans. Wireless Commun.*, vol. 4, no. 2, pp. 560–573, Mar. 2005.

[7] S. Gezici, H. Kobayashi, and H. V. Poor, "Nonparametric non line-of-sight identification," in *Proc. IEEE Vehicular Technology Conference*, vol. 4, 2003, pp. 2544–2548.

[8] S. Venkatesh and R. Buehrer, "Non-line-of-sight identification in ultra-wideband systems based on received signal statistics," *IET Microwaves, Antennas and Propagation*, vol. 1, no. 6, pp. 1120–1130, Dec. 2007.

[9] I. Guvenc, C.-C. Chong, and F. Watanabe, "NLOS identification and mitigation for UWB localization systems," in *Proc. IEEE Wireless Communications and Networking Conference (WCNC)*, Mar. 2007, pp. 1571–1576.

[10] S. Venkatesh and R. M. Buehrer, "NLOS mitigation using linear programming in ultrawideband location-aware networks," *IEEE Trans. Veh. Technol.*, vol. 56, no. 5, pp. 3182–3198, Sept. 2007.

[11] R. Battiti, A. Villani, and T. L. Nhat, "Neural network models for intelligent networks: deriving the location from signal patterns," in *Proc. Autonomous Intelligent Networks and Systems Symposium*, 2002.

[12] C. Nerguizian, C. Despins, and S. Affés, "Geolocation in mines with an impulse response fingerprinting technique and neural networks," *IEEE Trans. Wireless Commun.*, vol. 5, no. 3, pp. 603–611, Mar. 2006.

[13] M. Heidari, F. O. Akgül, N. A. Alsindi, and K. Pahlavan, "Neural network assisted identification of the absence of direct path in indoor localization," in *Proc. IEEE Global Telecommunication Conference (GLOBECOM)*, Nov. 2007, pp. 387–392.

[14] K. Pahlavan, X. Li, and J.-P. Mäkelä, "Indoor geolocation science and technology," *IEEE Communun. Mag.*, vol. 40, no. 2, pp. 112–118, Feb. 2002.

[15] M. Kanaan, M. Heidari, F. O. Akgül, and K. Pahlavan, "Technical aspects of localization in indoor wireless networks," *Bechtel Telecommun. Technical J.*, vol. 5, no. 1, pp. 47–58, Dec. 2006.

[16] K. Pahlavan, F. O. Akgül, M. Heidari, A. Hatami, J. M. Elwell, and R. D. Tingley, "Indoor geolocation in the absence of direct path," *IEEE Wireless Commun. Mag.*, vol. 13, no. 6, pp. 50–58, Dec. 2006.

[17] N. A. Alsindi, B. Alavi, and K. Pahlavan, "Measurement and modeling of UWB TOA-based ranging in indoor multipath environments," *IEEE Trans. Veh. Technol.*, vol. 58, no. 3, pp. 1046–1058, Mar. 2009.

[18] B. Alavi and K. Pahlavan, "Modeling of the distance error for indoor geolocation," in *Proc. IEEE Wireless Communications and Networking Conference (WCNC)*, vol. 1, Mar. 2003, pp. 668–672.

[19] B. Denis and N. Daniele, "NLOS ranging error mitigation in a distributed positioning algorithm for indoor UWB ad-hoc networks," in *Proc. IEEE International Workshop on Wireless Ad-Hoc Networks (IWWAN)*, May-June 2004, pp. 356–360.

[20] Y.-H. Jo, J.-Y. Lee, D.-H. Ha, and S.-H. Kang, "Accuracy enhancement for UWB indoor positioning using ray tracing," in *Proc. IEEE Position, Location, and Navigation Symposium (ION)*, Apr. 2006, pp. 565–568.

[21] N. A. Alsindi, B. Alavi, and K. Pahlavan, "Spatial characteristics of UWB TOA-based ranging in indoor multipath environments," in *Proc. IEEE International Symposium on Personal, Indoor, and Mobile Radio Communications (PIMRC)*, Sept. 2007.

[22] M. Heidari and K. Pahlavan, "A Markov model for dynamic behavior of ToA-based ranging in indoor localization," *EURASIP, European J. Advances in Signal Processing*, no. 241069, pp. 1–14, 2008.

[23] B. Alavi, "Distance measurement error modeling for time-of-arrival based indoor geolocation," Ph.D. dissertation, Worcester Polytechnic Institute, 2006.

[24] W. C. Davidon, "Variance algorithm for minimization," *Computer J.*, vol. 10, 1968.

[25] H. L. V. Trees, *Detection, Estimation, and Modulation Theory, Part I*, 1st ed. New York: John Wiley & Sons, Inc., 1968.

[26] H. V. Poor, *An Introduction to Signal Detection and Estimation*, 2nd ed. New York: Springer, 1998.
[27] Y. Qi, H. Kobayashi, and H. Suda, "Analysis of wireless geolocation in a non-line-of-sight environment," *IEEE Trans. Wireless Commun.*, vol. 5, no. 3, pp. 672–681, Mar. 2006.
[28] A. F. Molisch, "Statistical properties of the RMS delay-spread of mobile radio channels with independent Rayleigh-fading paths," *IEEE Trans. Veh. Technol.*, vol. 45, no. 1, pp. 201–204, Feb. 1996.
[29] H. Hashemi and D. Tholl, "Analysis of the RMS delay spread of indoor radio propagation channels," in *Proc. IEEE International Conference on Communciations*, vol. 2, 1992, pp. 875–881.
[30] T. S. Rappaport, S. Y. Seidel, and R. Singh, "900-MHz multipath propagation measurements for US digital cellular radiotelephone," *IEEE Trans. Veh. Technol.*, vol. 39, no. 2, pp. 132–139, May 1990.
[31] "Neural Network Toolbox, User's Guide." [Online]. Available: http://www.mathworks.com/access/helpdesk/help/pdf_doc/nnet/nnet.pdf
[32] T. Holt, J. F. Lee, and K. Pahlavan, "A graphical indoor radio channel simulator using 2D ray tracing," in *Proc. IEEE International Symposium on Personal Indoor and Mobile Radio Communications, PIMRC*, Sept. 1992, pp. 411–416.

Mohammad Heidari (mheidari@gmail.com) received his Ph.D. and M.Sc. degrees on challenges of indoor positioning systems and communication and computer networking concentrated on WiFi localization, respectively, at Center for Wireless Information Network Studies (CWINS) from Worcester Polytechnic Institute, Worcester, MA. His research interests are analysis dynamic behavior of WiFi and hybrid positioning systems, indoor geolocation applications, wireless sensor networks, UWB channel measurement and modeling. He is a member of IEEE.

Nayef Alsindi (S'02) received the B.S.E.E. degree from the University of Michigan, Ann Arbor, in 2000 and the M.S. degree in electrical engineering from Worcester Polytechnic Institute (WPI) , Worcester, MA, in 2004. He received his Ph.D. degree in electrical and computer engineering with the Center for Wireless Information Network Studies, Department of Electrical and Computer Engineering, WPI in 2008. From 2000 to 2002, he was a Technical Engineer with Bahrain Telecom. From 2002 to 2004, he was awarded a Fulbright Scholarship to pursue the M.S. degree at WPI. His research interests include performance limitations of time-of-arrival-based ultra wideband ranging in indoor non-line-of-sight (LOS) conditions, cooperative localization for indoor wireless sensor networks, and non-LOS/blockage identification and mitigation.

Kaveh Pahlavan (kaveh@wpi.edu) is a Professor of ECE, a Professor of CS, and Director of the Center for Wireless Information Network Studies, Worcester Polytechnic Institute, Worcester, MA. He is also a visiting Professor of Telecommunication Laboratory and Center for Wireless Communications, University of Oulu, Finland. He is the editor-in-chief of the INTERNATIONAL JOURNAL OF WIRELESS INFORMATION NETWORKS, a member of the advisory board of the IEEE WIRELESS MAGAZINE, a member of the executive committee of the IEEE PIMRC, a fellow of the IEEE since 1996, a Nokia fellow in 1999, and a Fulbright-Nokia scholar in 2000. He has served as the general chair and organizer of a number of successful IEEE events and has contributed to numerous seminal technical and visionary publications in wireless office information networks, home networking, and indoor geolocation science and technology. He is the principal author of *Wireless Information Networks* (with Allen Levesque), John Wiley and Sons, 1995, 2ed ed. 2005, and *Principles of Wireless Networks - A Unified Approach* (with P. Krishnamurthy), Prentice Hall, 2002. More details of his work are available at www.cwins.wpi.edu.